Carbon xerogels as supports for catalysts and electrocatalysts

Nathalie Job[1] *, Sandrine Berthon-Fabry[2], Stéphanie Lambert[1], Marian Chatenet[3], Frédéric Maillard[3], Mathilde Brigaudet[2], Jean-Paul Pirard[1]

[1] Laboratoire de Génie Chimique, Université de Liège, B6a, B-4000 Liège (Belgium)
[2] MINES ParisTech, CEP, BP 207, F-06904 Sophia-Antipolis Cedex (France)
[3] LEPMI, UMR 5631 CNRS/Grenoble-INP/UJF, BP75, F-38402 St Martin d'Hères Cedex (France)

** Corresponding author. E-mail : Nathalie.Job@ulg.ac.be*

Abstract. In order to improve mass transport in the pore texture of carbon supported catalysts, the widely used supports (activated carbons or carbon blacks) can be replaced by carbon gels, *i.e.* texture-tailored materials obtained by drying and pyrolysis of organic gels. Carbon xerogels issued from resorcinol-formaldehyde aqueous gels were used as metal catalyst supports both in gas phase heterogeneous catalysis and in PEM fuel cell electrodes. These materials, composed of very pure carbon, allow for excellent metal dispersion *via* impregnation methods. Pd-Ag/C catalysts were obtained by impregnation and tested for hydrodechlorination reactions in gaseous phase. Pt loaded carbon xerogels were tested as electrocatalysts in PEM fuel cell cathodes. In both cases, the well-adapted structure of the support proved to be a great advantage compared to classical activated carbons or carbon blacks: (i) in the gas phase reaction, diffusional limitations encountered with activated carbon supports were completely eliminated; (ii) in fuel cells, Pt loaded catalysts enabled decreasing the effect of diffusion in the catalytic layer on potential loss and led to increasing drastically the global metal utilization ratio.

1. Introduction

Porous carbon materials are widely used in many applications: adsorption in liquid or gas phase [1], gas separation [2], supports for catalysts [3], electrocatalysis [4], materials for batteries [5], etc. In all these processes, the pore texture of the chosen carbon material plays a major role. Indeed, adsorbates and reactants must circulate within the pore texture. The control of the carbon pore texture is thus a key to an efficient process.

However, carbons used in industrial applications and in electrochemical devices, such as activated carbons or carbon blacks, most often display quite inappropriate pore textures. In the case of activated carbons, for instance, the pore texture obtained after thermal treatment of the natural source (wood, coal, nutshells, …) is completely dependent on the nature of the precursor. The variability in feedstock can lead to reproducibility problems in terms of pore texture and chemical properties. Moreover, activated carbons are generally microporous, with low macropore or mesopore volumes [6], which often induces diffusional limitations during (electro)catalytic and adsorption processes. Carbon blacks [7], obtained by partial combustion or thermal cracking of hydrocarbons, have also been used in numerous applications, and remain the elected material for fuel cell electrodes [4]. These carbons are composed of microporous near-spherical particles of colloidal sizes (~ 20 – 60 nm), coalesced together as aggregates (1 – 100 µm). Although catalysts supported on carbon blacks lead to very satisfactory results at the laboratory scale, the small particle size is an important drawback for large-scale applications: in the case of fixed bed reactors or fuel cells, for instance, the global pore texture is then defined by the packing of the carbon aggregates, which depends on the carbon implementation.

These drawbacks call for the development of carbon materials with controllable and tunable pore texture. In addition, and especially for electrochemical applications, high purity of the carbon supports is essential [4]. This is why recent works were dedicated to the preparation of synthetic porous carbon materials, with special attention to the control of the textural properties. Several routes were investigated in the last 20 years. Among the numerous new carbon materials developed, carbon gels, *i.e.* carbon xerogels, aerogels and cryogels, prepared by drying and pyrolysis of organic gels, have been extensively studied [8-12]. These nanostructured carbons were quite recently envisaged as an alternative to other materials in gas or liquid phase heterogeneous catalysis [13-15] or in Proton Exchange Membrane (PEM) fuel cell electrodes [16-20]. PEM fuel cell electrodes can be considered as micro reactors composed of Pt/carbon catalyst particles, interparticle voids and ionomer (Nafion®, usually) [4]. The principles of heterogeneous catalytic reactors design apply to this system, though the

reaction and transport phenomena are complicated by the presence of liquid water and gas, and by the necessary contact of the active phase (Pt) with its support and the ionomer connected to the membrane.

The aim of this work is to show the advantages of carbon xerogels as catalyst supports in general, and more precisely as electrocatalyst supports for PEM fuel cell electrodes. To this aim, carbon xerogel supports with various pore textures were prepared and tested both in gas phase heterogeneous catalysis (hydrodechlorination of CH_2Cl-CH_2Cl into ethylene on Pd-Ag/C catalysts) and in electrocatalysis (air/H_2 PEM fuel cell cathode). The results parallel the interest of these materials as catalyst support in gas phase catalysis and in electrochemical applications from the mass transport point of view.

2. Experimental Methods

2.1. Synthesis of carbon xerogels

In this work, several carbon xerogels with different pore texture (*i.e.* pore size and pore volume) were selected. It was demonstrated that modifying the pH of the precursor solution leads to the obtaining of final carbon supports with various pore textures [8-12]. Carbon gels are composed of interconnected near-spherical nodules, the size of which depends on the precursor solution composition, the pH being a key variable. By changing the pH of the resorcinol-formaldehyde solution, one can modify the size of the nodules and thus the size of the pores after drying and pyrolysis (Figure 1). So, according to these results, the pore size was adjusted between 25 and 300 nm. In the case of PEM fuel cell cathodes, the performance of carbon xerogels was compared to that of an aerogel (*i.e.* dried by supercritical drying) prepared following a method used in a previous work [17].

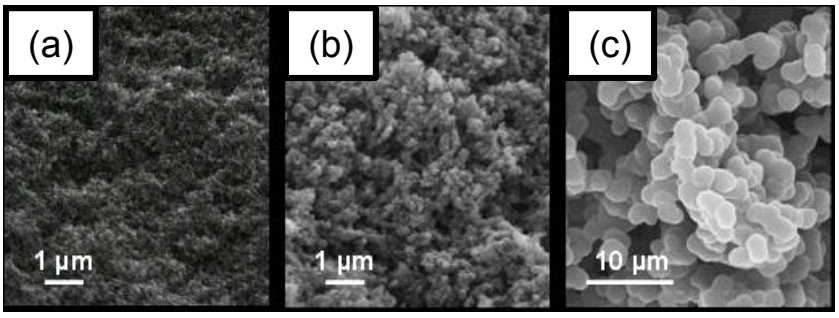

Fig. 1 : Morphology of carbon xerogels prepared at various pH: (a) pH = 6.50, (b) pH = 6.00, (c) pH = 4.00. The size of the carbon nodules is completely determined by the composition of the RF solution, and does not depend on the drying technique. However, the drying method may alter the material texture by shrinkage upon drying.

Briefly, carbon xerogels were prepared by evaporative drying and pyrolysis of resorcinol-formaldehyde gels, following a method extensively described elsewhere [12]. The wet gels were first obtained by polycondensation of resorcinol with formaldehyde in water, in the presence of Na_2CO_3 as basification agent. Different polymer textures were achieved by modifying the pH of the precursor solution: to this aim, the resorcinol/sodium carbonate molar ratio, *R/C*, was fixed between 250 and 2000. Both the dilution ratio, *D*, *i.e.* the solvents/(resorcinol + formaldehyde) molar ratio, and the resorcinol/formaldehyde molar ratio, *R*/*F*, were kept constant (5.7 and 0.5, respectively). Note that, in *D*, the term "solvents" regroups the deionised water added but also water and methanol (stabilizer) included in the formaldehyde solution. The wet materials were dried without any pre-treatment in a vacuum oven, at 60°C, by decreasing the pressure from 10^5 Pa to 10^3 Pa over two days. The samples were then left at 150°C (10^3 Pa) for 12 h. Finally, carbon xerogels were obtained by pyrolyzing the dry materials for 2 h at 800°C under nitrogen flow [11, 12]. The pore texture of all the supports, used in other studies, was analyzed using nitrogen adsorption-desorption, mercury porosimetry and helium pycnometry [11, 12].

2.2. Synthesis of metal catalysts supported on carbon xerogels

For gas phase heterogeneous catalysis applications, bimetallic Pd-Ag/carbon xerogel catalysts were obtained by impregnation of pellets with palladium and silver nitrate, as detailed in reference [14]. The metal concentration of the various impregnating solutions were calculated so that the nominal Pd and Ag content was equal to 1.5 wt.% for both metals, depending on the pore texture of the support, and assuming that all the metal entering the pore texture remains after drying and reduction. Carbon pellets were immersed in the corresponding solution for 24 h. The samples were then filtered in order to remove the excess of solution and dried under flowing air at ambient temperature for 24 h. The drying process was completed by vacuum drying (24 h, 150°C). After drying, the samples were reduced for three hours in flowing H_2 at 350°C (H_2 flowrate: 0.025 mmol s^{-1}, heating rate: 350 °C h^{-1}). The pellets were then crushed and sieved in order to obtain four samples of each catalyst with decreasing mean pellet size. The meshes of the sieves were 1.250, 1.000, 0.710, 0.500 and 0.250 mm wide.

For electrochemical applications (PEM fuel cell cathodes), Pt/C catalysts were prepared. Very good Pt dispersion can be obtained *via* several impregnation methods [14, 15, 21], but the metal weight percentage of these catalysts (< 5 wt.%) is not high enough for applications in PEM fuel cells, especially in the case of cathodes of air/H_2 devices. Indeed, in order to minimize ohmic and transport losses within the electrode, and to compensate for both the sluggish oxygen reduction reaction rate and the usual lack of contact between Pt and the ionomer (see §3.3), two antagonistic conditions must be fulfilled: (i) the thickness of the catalytic layer must be low enough, and (ii) the metal loading of the electrode must be high enough. This naturally implies the selection of catalysts with high metal weight percentage (usually, 20 to 80 wt.% [4]). So as to achieve high Pt weight percentages, two methods were used. The first one, developed by Marie *et al*. [16-19], consists in: (i) impregnation of the support with a diluted H_2PtCl_6 aqueous solution, followed by (ii) direct metal reduction in liquid phase with $NaBH_4$, (iii) drying in air (60°C, 12 h) and (iv) reduction under H_2 (350°C, 30 min). The second one, the so-called 'Strong Electrostatic Adsorption' (SEA) method [22], consists in an impregnation during which the electrostatic interactions between the metal precursor and the support are maximized by adjusting the pH of the carbon/water/Pt precursor slurry to the adequate value. This value depends on both the surface chemistry of the support and the nature of the Pt precursor. In the case of the impregnation of carbon xerogels with H_2PtCl_6 aqueous solutions, the initial pH leading to the highest Pt uptake was found to be 2.5 [23]; the corresponding maximum Pt loading was ranging from 8 to 10 wt.% while keeping very small Pt particles after reduction under H_2 flow at temperatures ranging from 200 to 450°C [23-24]. Pt/C catalysts with high dispersion were then prepared in SEA conditions, *i.e.* at pH = 2.5, following the method described in previous works [23-24]. In order to increase the metal weight percentage, the impregnation/reduction/drying cycle was repeated up to three times.

2.3. Catalyst characterization

Actual metal contents were determined by inductively coupled plasma-atomic emission spectroscopy (ICP-AES). Metal particles were examined by X-ray diffraction (XRD), transmission electron micrography (TEM) and CO chemisorption. Details about the specific procedures used can be found elsewhere [23-24]. In the case of Pd-Ag/C catalysts, the combination of these three techniques enabled us to check that the alloy particles size as well as their bulk and surface composition remained constant, whatever the support used [14].

The electrochemically active Pt surface area of the Pt/C catalysts was determined by CO stripping on a rotating disk electrode (EDT 101, Tacussel). The experiments were carried out on a thin active layer (AL) of Pt/C catalyst deposited onto a glassy carbon electrode. The electrode and AL preparation are described in ref [25]. CO stripping measurements were carried out in sulphuric acid (1 M, Suprapur-Merck) at 25 °C, using an Autolab-PGSTAT20 potentiostat with a three-electrode cell and a saturated calomel electrode (SCE) as reference (+0.245 V *vs.* normal hydrogen electrode, NHE). All the potentials are expressed on the NHE scale hereafter. The Pt surface was saturated with CO (N47, Alphagaz) by bubbling for 6 min in the solution; afterwards, the non-adsorbed CO was removed from the cell by Ar bubbling for 39 min. During the CO

adsorption and Ar bubbling, the electrode was held at +0.095 V *vs.* NHE. Voltammetric cycles were then recorded at 0.02 V s^{-1} between +0.045 and +1.245 V *vs.* NHE. The active area of platinum, $S_{CO\text{-}strip}$, was calculated assuming that the electrooxidation of a full monolayer of CO_{ads} requires 420×10^{-6} C $cm^{-2}{}_{Pt}$ [26].

2.4. Catalytic tests – gas phase heterogeneous catalysis

Hydrodechlorination of 1,2-dichloroethane into ethylene was performed in a fixed bed reactor. The measurement device is completely described in reference [14]. Feed gas flows were kept constant by mass flow controllers: 0.459 mmol s^{-1} helium and 0.025 mmol s^{-1} hydrogen. The 1,2-dichloroethane flow was equal to 0.012 mmol s^{-1}. These conditions ensure that no external mass transfer limitations occur. The 1,2-dichloroethane consumption rate was measured with each catalyst at 350°C and at 0.3 MPa for 3 h, which ensured stabilization. The effluent of the reactor was analyzed by gas chromatography with a flame ionization detector (FID). Only C_2H_4 and C_2H_6 concentrations were used in this study due to the too large imprecision of $CH_2Cl\text{-}CH_2Cl$ concentration measurements: indeed, since 1,2-dichloroethane is liquid at room temperature, condensation could occur in the pipes before injection in the FID device. The measurements were repeated with the four pellet sizes for every catalyst. The catalytic bed was constituted of 200 mg of non-reduced Pd-Ag/C catalyst pellets. Prior to the measurement, the catalyst was reduced *in situ*: under flowing hydrogen (0.025 mmol s^{-1}) and at a pressure of 0.125 MPa, the catalyst was heated from room temperature to 350°C at a rate of 350 °C h^{-1} and was maintained at 350°C for 3 h.

2.5. Electrocatalytic tests – PEM fuel cell cathode

Pt/C catalysts, prepared either by impregnation followed by reduction in liquid phase [16-19] or by the SEA method [23-24], were tested in PEM fuel cell cathodic catalytic layers in order to compare their respective performance. The powdered catalysts were used to prepare 50 cm² MEAs, which were further tested on a unit monocell test bench. The MEA preparation method, the test device and the measurement procedure are completely described in reference [18]. Briefly, the MEAs were prepared by the decal method [17-19], which consists of spraying an ink composed of Pt/carbon catalyst, water and ionomer (Nafion®) onto a support, *i.e.* a Kapton® sheet; afterwards, the electrolyte, *i.e.* a Nafion® membrane, and the anode (commercial, Paxitech), composed of a Pt-doped carbon black deposited onto a carbon felt, are piled up on the sprayed layer. The whole assembly is further hot-pressed to compose the MEA. For comparison, the catalytic layer thickness of the cathode was chosen equal as in reference [18]. The Nafion®/carbon mass ratio of the ink used to prepare the MEAs, *N/C*, was fixed at 0.5. After a standardized start-up procedure, polarization curves, *i.e.* the $E_{cell} = f(i)$ curves, were measured by setting the cell voltage at each desired value for 15 min, which assured the stabilization of the current intensity. Since the Pt content of all catalysts is not the same (impregnation and reduction in liquid phase: 30-35 wt.%; SEA method: 15 wt.%), the current was normalized with either the geometric area of the electrode (i_s) or the Pt metal loading of the cathode (i_m).

3. Results and Discussion

3.1. Catalyst characterization

The complete characterization data of Pd-Ag/carbon xerogel catalysts prepared by impregnation with silver and palladium nitrates are available in reference [14]. To summarize, these catalysts display Pd-Ag alloy particles about 3-4 nm in size. The constancy of the alloy particle bulk and surface composition was checked by CO chemisorption and XRD measurements. Results show that these parameters do not depend on the pore texture of the support. In all cases, the Pd-Ag particles are composed of 50-55 at.% Pd. Because of the lower surface energy of Ag in comparison with Pd, silver enrichment at the particle surface occurs and the surface composition is about 10 at. % Pd. So, except for the pore size and pore volume of the support, the catalysts

tested in 1,2-dichloroethane hydrodechlorination can be considered as equivalent and can be compared to each other.

Characterization of Pt/carbon xerogel catalysts show that impregnation with H_2PtCl_6 followed by liquid phase reduction in order to achieve about 30 wt.% metal in one single step leads to poorly dispersed catalysts (Figure 2a). The catalysts are bimodal: small particles (2-7 nm) are surrounded by larger ones (10-30 nm). In our opinion, the two particle families originate from two different mechanisms of Pt particles formation: (i) the small particles are mostly formed by adsorption of $PtCl_6^{2-}$ anions on the support surface followed by reduction in the adsorbed state while (ii) the large particles are probably originating from the direct reduction of $PtCl_6^{2-}$ anions located in the impregnation solution, followed by metal precipitation onto the carbon support. Indeed, the adsorption of $PtCl_6^{2-}$ anions onto the carbon surface is limited by a thermodynamic equilibrium which depends on the carbon surface chemistry and on the pH of the impregnation solution. So, impregnation performed at the optimal pH value (*i.e.* under SEA conditions), followed by elimination of the excess solution, drying and reduction under hydrogen (200°C, 1h) leads to very well dispersed catalysts (Figure 2b). However, the metal content is limited to about 8 wt.% by the adsorption equilibrium [23]: it is not possible to increase the amount of Pt deposited without altering the excellent metal dispersion obtained, which explains the poor metal dispersion obtained when 30 wt.% Pt catalysts were prepared in one single impregnation step by using liquid-phase reduction. So as to increase the Pt content of the catalyst while keeping an excellent metal dispersion, one must repeat the impregnation/drying/reduction cycle using the SEA method [24]. This does not alter the metal dispersion: Figure 2c shows indeed that consecutive impregnation steps lead to increasing regularly the Pt weight percentage without modifying the average metal particle size (~2 nm).

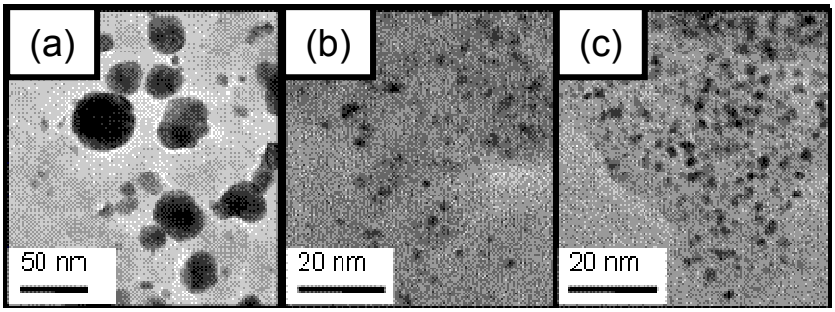

Fig. 2 : Pt/carbon xerogel catalysts prepared on the same support (pore size range: 50 - 85 nm, pore volume = 2.1 $cm^3\ g^{-1}$): (a) impregnation with H_2PtCl_6 followed by direct reduction in liquid phase with $NaBH_4$ (30 wt.% Pt [18]); (b) SEA method, one impregnation (7.5 wt.% Pt [23, 24]); (c) SEA method, three successive impregnations (22.7 wt.% Pt [24]).

Figure 3 shows the CO_{ads} voltammograms of three catalysts prepared on the same support, *i.e.* a carbon xerogel with small macropores (50-85 nm, pore volume = 2.1 $cm^3\ g^{-1}$). The three catalysts were obtained either by: (i) impregnation with H_2PtCl_6 and reduction in liquid phase by $NaBH_4$ (30 wt.%, bimodal, see Figure 2a) or (ii) double impregnation with H_2PtCl_6 in SEA conditions and reduced under H_2 at 200°C during 1h (15.0 wt.%) or (iii) double impregnation with H_2PtCl_6 in SEA conditions and reduced under H_2 at 450°C during 5h (15.0 wt.%). Note that, since the Pt weight percentage of the catalysts is not the same, and because the current measured is reported per mass unit of Pt, the signal corresponding to the support is lower for the first catalyst. CO_{ads} electrooxidation on Pt proceeds *via* a Langmuir-Hinshelwood mechanism, which includes water dissociation into oxygen-containing species, and recombination of the former species with CO, yielding CO_2 [27]. The electrooxidation of a CO_{ads} monolayer is a structure-sensitive reaction and provides a wealth of information on the particle size distribution and the presence/absence of particle agglomeration [27-29].

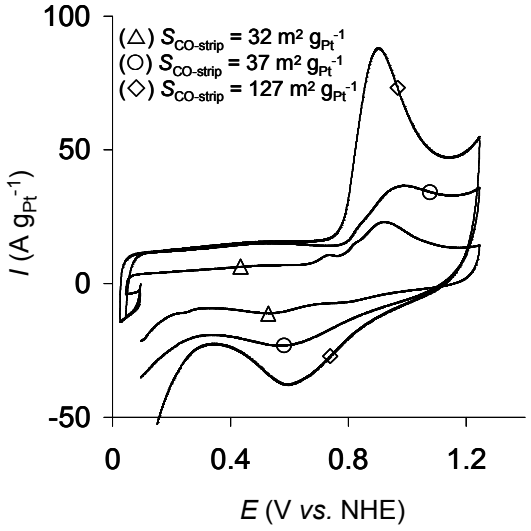

Fig. 3 : CO_{ads} stripping voltammogram on carbon xerogel supported Pt catalysts in H_2SO_4 (1 M) at 25°C; sweep rate of 0.02 V s^{-1}. Support with small macropores (50-85 nm, pore volume = 2.1 cm^3 g^{-1}). (△) Catalyst prepared by impregnation with H_2PtCl_6 and reduced in liquid phase [18]; (○) catalyst prepared by double-impregnation using the SEA method, reduced at 200°C (H_2, 1 h), (◇) catalyst prepared by double-impregnation using the SEA method, reduced at 450°C (H_2, 5 h).

The catalyst prepared by impregnation and liquid-phase reduction presents three oxidation peaks centred at about +0.73, +0.81 and +0.92 V *vs*. NHE, corresponding to CO_{ads} electrooxidation at Pt particle agglomerates, large Pt particles (d > 3.3 nm) and small Pt nanoparticles (d ~ 1.9 nm), respectively [25]. This agrees with TEM observations, which show that the particle size distribution of the catalyst is bimodal: large particles (10-30 nm) and smaller particles (2-5 nm). The corresponding active Pt surface, $S_{CO\text{-}strip}$, equals 32 m^2 g_{Pt}^{-1}. In the case of the two other samples, prepared by double impregnation following the SEA method, one major peak is observed, and a second one, located around +0.81 V *vs.* NHE being barely visible. Concerning these curves, two observations can be made. First, the corresponding Pt surfaces are very different: $S_{CO\text{-}strip}$ = 37 m^2 g_{Pt}^{-1} (reduction at 200°C) *vs.* $S_{CO\text{-}strip}$ = 127 m^2 g_{Pt}^{-1} (reduction at 450°C). Second, the major peaks are not centred at the same potential value: *ca.* +1.00 V *vs.* NHE (200°C) and +0.91 V *vs.* NHE (450°C). This can be explained by Cl poisoning of the Pt surface when the reduction temperature is too low (200°C). Indeed, this trend is easily reproducible with a commercial electrocatalyst with a similar Pt particle size (*ca.* 2 nm) in Cl-containing electrolyte. The positive shift of the onset of the CO electrooxidation peak may be ascribed to the competition between water and chloride species for adsorption sites. Indeed, both experimental [29] and computational modelling studies [30] have suggested that there are only a fixed number of active sites on the Pt surface, which are able to form OH species and to initiate the CO electrooxidation. Competitive adsorption by Cl^- species will thus decrease artificially the number of active sites and shift both the onset and the main CO electrooxidation peak towards positive potentials. This demonstrates the importance of the reduction treatment on the catalyst; in future works, non-chlorinated Pt precursors should be investigated.

Note that Cl poisoning is also detectable by CO chemisorption measurements, but the phenomenon is less visible than in the case of CO stripping [24]. Indeed, in this former technique, CO adsorption equilibrium is reached prior to any further gas injection. So, chlorine adsorbed at the surface of the Pt particles is partially displaced by CO, which is one of the strongest Pt poisons [31]. On the contrary, in the case of CO stripping, the kinetics of displacing may be too slow to be completed within a few minutes: as a consequence, surfaces detected by CO chemisorption on Cl-poisoned Pt catalysts are larger than those obtained by CO stripping [24].

3.2. Gas phase heterogeneous catalysis

The ability to control finely the pore size in carbon gels is a great advantage compared to classical activated carbons, the pore texture of which is mainly fixed by the origin of the raw material and usually composed of a large fraction of very small pores (micropores, size < 2 nm). On the contrary, the presence of large volumes of meso- or macropores in carbon xerogels and aerogels can minimize, or even suppress the diffusional limitations often encountered in heterogeneous catalysis processes. As an example, Figure 4 reports results of hydrodechlorination of 1,2-dichloroethane performed over Pd-Ag bimetallic catalysts supported on carbon xerogels of various pore size (from small mesopores, 8-10 nm, to macropores, 60-70 nm). In order to highlight the existence of diffusional limitations, the pellet size was increased from 200 to 1200 µm, and the effectiveness of the catalyst, *i.e.* the ratio between the measured reaction rate and the intrinsic reaction rate obtained in absence of diffusional limitations, was evaluated. As a result (Figure 4), the effectiveness of the catalyst supported on the carbon xerogel with 10 nm pores decreased with the pellet size, like in the case of an activated carbon supported catalyst, whereas no decrease was observed for the macroporous support (60-70 nm). Calculations show that, in the latter case, the catalyst remains free of diffusional limitations for pellet sizes up to 40 mm at 350°C and 70 mm at 300°C. In the case of the activated carbon, a fine powder should be used to get rid off internal diffusional limitations, which is not possible in fixed beds due to the pressure drop. On the contrary, pellets of reasonable size can be used in the case of macroporous carbon xerogels.

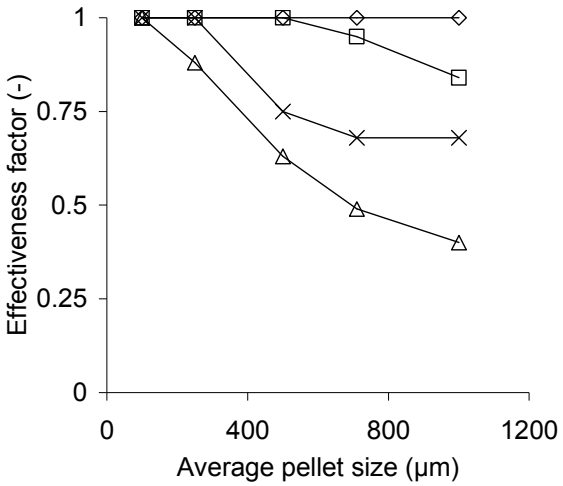

Fig. 4 : Hydrodechlorination of CH_2Cl-CH_2Cl over Pd-Ag/carbon catalysts at 350°C in a fixed bed reactor: effectiveness factor as a function of the pellet size. Carbon xerogel supported catalysts: (△) small mesopores (8-10 nm), (□) large mesopores (25-30 nm), (◇) macropores (60-70 nm). Catalyst supported on a microporous activated carbon (×). Data adapted from [14].

3.3. PEM fuel cell cathode

The advantages of carbon gels in heterogeneous catalysis can be transferred to electrochemical devices such as PEM fuel cells. As shown in Figure 5a, the catalytic layer of a PEM fuel cell is composed of Pt/carbon catalyst particles, interparticle voids and ionomer, hot-pressed between a proton-exchange membrane and a diffusion layer (carbon felt) [4]. Thus, a catalytic layer of a PEM fuel cell constitutes a microreactor of heterogeneous catalysis where mass transports are complicated by: (i) the presence of two fluid phases (gas and condensed water), and (ii) the proton transport *via* the ionomer network (Nafion®, usually). Indeed, to be active, the metal (Pt) catalyst particles must be in contact with the carbon support and connected to the membrane *via* the ionomer. In addition, reactants and products must circulate easily through the catalytic layers: (i) the catalyst

must be reached by the gas reactant (H_2 or O_2), which percolates through the porous structure of the catalytic layer; (ii) protons and electrons have to be collected by the ionomer (Nafion®) and the catalyst support, respectively, and driven to the membrane (protons) and the current collector (electrons); (iii) water must be transported to the membrane for humidification, and the excess eliminated to avoid electrode flooding. Typically, carbon blacks are used for the preparation of the catalysts. However, the packing of the carbon particle aggregates, and therefore the pore structure of the catalytic layers, depends on the carbon black nature and on the electrode processing. Typically, at the air-fed cathode, where oxygen, proton and water transports are involved in the oxygen reduction reaction, high potential losses due to diffusional limitations offset the cell performance [32]. These limitations are compensated by the use of catalytic layers with high Pt loading, which increases the cost of the electrode. In addition, a large fraction of the Pt may be inactive due to a lack of contact between Pt and Nafion® (lack of ionic percolation), and to the presence of liquid water within the pores of the cathode (liquid water-induced mass-transport limitation).

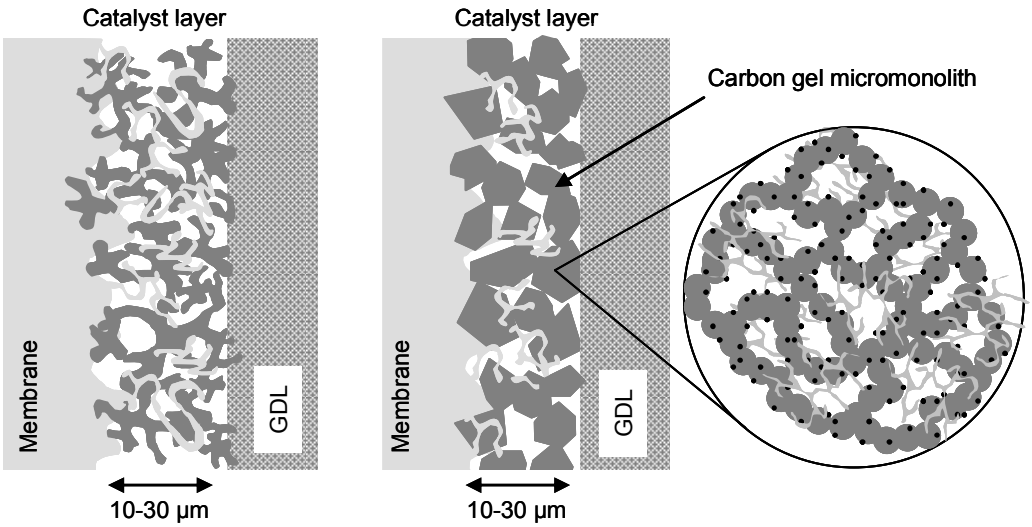

Fig. 5 : Structure of a PEM fuel cell electrode: membrane, catalyst layer and gas diffusion layer (GDL). (a) Carbon black as catalyst support: the catalytic layer is composed of aggregates of loosely bonded carbon black particles containing Pt; (b) carbon gel as catalyst support: the catalytic layer is composed of carbon gel micromonoliths made of a rigid 3D structure, insensitive to compression and with a defined pore texture. The Nafion® network and Pt particles are represented in light grey and black, respectively.

The development of new catalytic layer structures should induce cost reduction *via* the decreasing of the diffusion-induced potential losses. In this latter field, carbon aerogels and xerogels constitute an interesting alternative to carbon blacks because their meso/macropore texture is totally independent on the electrode processing and can be regulated by choosing correctly the composition of the pristine wet gel; besides, the high purity of carbon gels ensures the absence of pollutants inherent to the support origin and detrimental to the electrocatalytic activity. In the electrode structure, the carbon black particle agglomerates are replaced by micromonoliths of carbon gel made of covalently bonded carbon nodules (see §2.1), which preserves the pores located in-between (Figure 5b).

The total voltage loss of the cell with regard to the reversible H_2/O_2 cell voltage can be decomposed into several components [33]: (i) the cathode overpotential, η_{ORR}, due to the slowness of the O_2 reduction kinetics; (ii) the ohmic losses, η_{Ohm}, due to the resistance of the proton migration through the membrane, the electronic contact resistances between the flow-fields plates and the diffusion media, and the contact between the carbon grains; (iii) the mass-transport losses, or 'diffusion overpotential', η_{diff}, induced by slow O_2 diffusion through the

diffusion layer and the catalytic layer. In such systems, kinetic and mass transport losses of the anode can be neglected [33]. One can write:

$$E_{cell} = E_{rev}[p(H_2), p(O_2), T] - \eta_{ORR} - \eta_{Ohm} - \eta_{diff} \quad (1)$$

where E_{rev} is the reversible H_2/O_2 cell voltage, $p(H_2)$ and $p(O_2)$ are the reactant partial pressures in the anode and cathode, and T is the temperature of the cell. The first two contributions to the voltage loss can be measured. Briefly, η_{ORR} is obtained from measurements at low current densities, *i.e.* from data obtained in the near-absence of mass transport limitations and ohmic resistance; η_{Ohm} is obtained by measurement of the ohmic resistance of the cell by impedance spectroscopy, performed *in situ*. Finally, all the other terms of eq. (1) being known, η_{diff} can be deduced.

As an example, Figure 6 shows the contribution of diffusion to the voltage loss of several MEAs working in an air/H_2 monocell device at 70°C and prepared with carbon xerogels as supports. For comparison, the result obtained using a carbon aerogel with a completely different pore texture is also reported. In all cases, the Pt/C catalysts were prepared by impregnation with H_2PtCl_6 followed by reduction in liquid phase with $NaBH_4$, as described in §2.2. All conditions (thickness, Nafion® content of the catalytic layer, pretreatments, Pt dispersion and morphology, etc.) were kept identical, except for the nature of the carbon support for the Pt nanoparticles. One can clearly observe that the diffusion overpotential depends on the pore size: in the xerogel series, η_{diff} decreases regularly when the pore size increases. However, both the pore size and the void fraction of the support play a role in mass transport. This explains why the aerogel, the maximum pore size of which is about 25 nm, displays diffusion overpotential equivalent to that of the xerogel with the largest pore size (250-300 nm): indeed, the pore volume of the aerogel is more than twice that of the xerogel (4.8 $cm^3\ g^{-1}$ *vs.* 2.2 $cm^3\ g^{-1}$). These results show how tuning the pore size of the catalyst support may decrease the limitations due to mass transport, exactly like in gas phase heterogeneous catalysis.

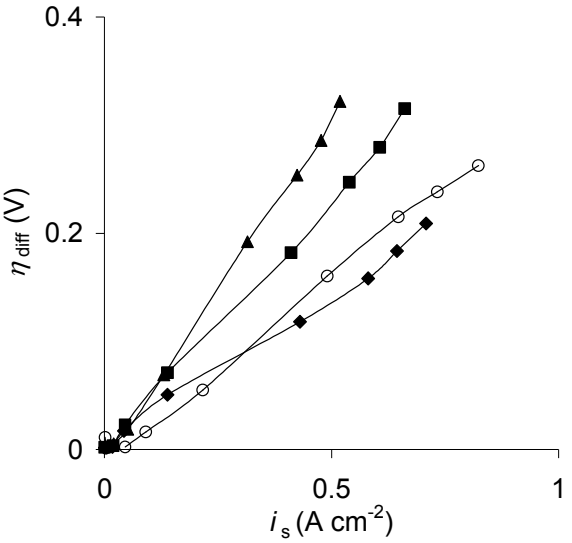

Fig. 6 : Diffusion overpotential *vs.* experimental current density per surface unit of electrode. MEAs prepared with different carbon gel supports at the cathode: (▲) mesoporous carbon xerogel (30-40 nm, 1.3 $cm^3\ g^{-1}$), (■) carbon xerogel with small macropores (50-85 nm, 2.1 $cm^3\ g^{-1}$), (◆) carbon xerogel with large macropores (250-300 nm, 2.2 $cm^3\ g^{-1}$), (○) mesoporous carbon aerogel with small mesopores (15-25 nm, 4.8 $cm^3\ g^{-1}$).

Besides mass transport, the cathode performance can be increased by increasing the global utilization ratio of Pt. Indeed, up to 90% of the platinum particles of a catalytic layer may be inactive, because of diffusional

limitations in the catalytic layer or because the truly active Pt surface is low [34]. The latter problem is due to the fact that many particles are not in contact with the electrolyte (Nafion®), and to metal agglomeration observed in catalysts with high metal weight percentage. Figure 7 compares the mass activity of catalysts prepared on various supports and with different Pt deposition methods. One can observe that increasing the metal dispersion by using the SEA method instead of impregnation followed by reduction in liquid phase (§2.2) allows increasing the cathode performance in terms of Pt mass activity: in the case of the carbon xerogel support, the current produced per mass unit of Pt, i_m, is almost doubled when the SEA technique is used, which is attributed to the elimination of large Pt particles and aggregates obtained by impregnation and liquid phase reduction. Finally, the performances of the carbon xerogel supported Pt catalysts prepared by the SEA method can be compared to that obtained with a commercial cathode prepared from Pt/carbon black. The commercial and home-made electrodes display rather identical performances in the so-called 'kinetic' region ($i < 1$ kA g_{Pt}^{-1}), where the mass transport limitations are negligible. This behaviour indicates that the intrinsic mass activity of the Pt nanoparticles in these two types of electrodes are close, exhibiting no dramatic difference of Pt particles morphology. On the contrary, in the mass transport controlled region ($i > 1$ kA g_{Pt}^{-1}), the performance, in terms of Pt utilization, is clearly higher in the case of the SEA catalyst supported on carbon xerogel. Such performance enhancement is attributed to: (i) the decrease of mass transport limitations, and (ii) the improvement of Pt-Nafion® contact, all inherent to the carbon support texture.

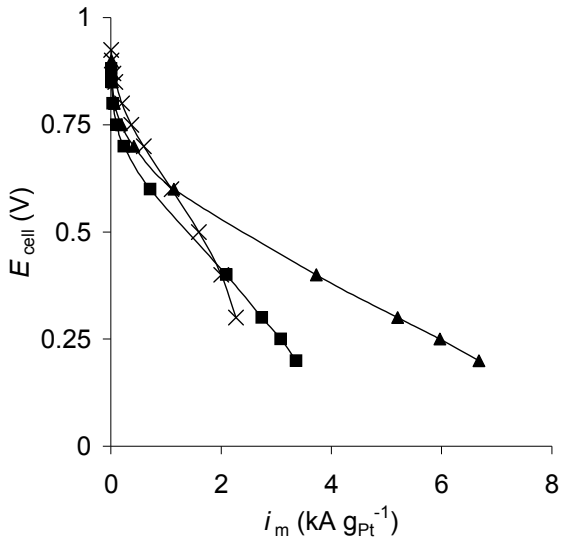

Fig. 7 : Cell voltage *vs.* Pt mass activity. (■) carbon xerogel with small macropores (50-85 nm, 2.1 cm^3 g^{-1}), impregnation + liquid phase reduction [18]; (▲) carbon xerogel with small macropores (50-85 nm, 2.1 cm^3 g^{-1}), SEA method (double impregnation, reduction under H_2 flow at 450°C [24]), (×) commercial cathode (Pt/carbon black, Paxitech).

4. Conclusion

Nanostructured carbon materials can be obtained by drying and pyrolysis of resorcinol-formaldehyde aqueous gels. The pore texture is regulated by both the gel synthesis conditions and the drying procedure, and a wide spectrum of pore textures can be obtained. In particular, the pore size can be adjusted with regard to the final application. In addition, these materials are composed of very pure carbon, and are quite suitable to the preparation of highly dispersed metal catalysts with high metal weight percentage.

The main advantage of such materials, *i.e.* the possibility to minimize mass transfer limitations during a reaction performed on a carbon-supported catalyst, can be transferred from gas-phase heterogeneous catalysis to

electrocatalysis. The effect of the pore texture is clearly observed in a PEM fuel cell (monocell test bench) in which the cathodic catalytic layer is prepared from Pt/carbon gel catalysts. Like in gas-phase heterogeneous catalysis, the pore size and void fraction of the catalyst support are determining in the mass transport phenomena, and both textural parameters can be tuned *via* the pristine gel composition and drying procedure. Carbon xerogels, which are the easiest to prepare, can lead to performance close to that of carbon aerogels provided that the pore size and volume are large enough. However, the optimal pore texture has not been determined yet. Since the pore texture range of carbon aerogels is wider than that accessible to carbon xerogels [12], the formers should not be abandoned despite the complexity of the drying process. In future works, the performance of the fuel cell electrodes will be optimized with regard to the Nafion® and Pt content of the catalytic layers, and to the humidity ratio of the feeding air and hydrogen.

Acknowledgements

N.J. and S.L. thank the F.R.S.-FNRS (Belgium) for postdoctoral researcher grants. The Belgian authors thank the Fonds de Recherche Fondamentale Collective, the Ministère de la Région Wallonne and the Interuniversity Attraction Pole (IAP-P6/17) for their financial support, and acknowledge the involvement of their laboratory in the Network of Excellence FAME of the European Union Sixth Framework Program. The French authors thank the Groupement des Écoles des Mines (GEM).

References

[1] F. Rodríguez-Reinoso, A. Sepúlveda-Escribano, in *Handbook of Surfaces and Interfaces of Materials*; Nalwa, H.S., Ed.; Academic Press, San Diego, 2001, pp. 309-355.
[2] A. Bailey, in *Porosity in Carbons*; Patrick, J.W., Ed.; Wiley, UK, 1995, pp. 209-226.
[3] F. Rodríguez Reinoso, A. Sepúlveda-Escribano, in *Carbon Materials for Catalysis*; Serp, P., Figueiredo, J.L., Eds.; Wiley, New York, 2009, pp. 131-156.
[4] F. Maillard, P. Simonov, E. R. Savinova, in *Carbon Materials for Catalysis*; Serp, P., Figueiredo, J.L., Eds.; Wiley, New York, 2009, pp. 429-481.
[5] F. Béguin, E. Frackowiak, in *Handbook of Nanomaterials*; Gogotsi, Y., Ed.; CRC Press, Boca Raton (FL), 2006, pp. 713-737.
[6] J.F. Byrne, H. Marsh, in *Porosity in Carbons*; Patrick, J.W., Ed.; Wiley, UK, 1995, pp.1-66.
[7] M.H. Hess, C.R. Herd, in: *Carbon Black*; Donnet, J.B., Bansal, R.C., Wang, M.J., Eds.; Marcel Dekker, New York, 1993, pp. 89-174.
[8] R.W. Pekala, J. Mater. Sci. **24** (1989) 3221.
[9] R.W. Pekala, C.T. Alviso, J.D. LeMay, in *Chemical Processing of Advanced Materials*; Hench, L.L., West, J.K., Eds.; Wiley, New York, 1992, pp. 671-683.
[10] S.A. Al-Muhtaseb, J.A. Ritter. Adv. Mater. **15** (2003) 101.
[11] N. Job, R. Pirard, J. Marien, J.-P. Pirard, Carbon **42** (2004) 619.
[12] N. Job, A. Théry, R. Pirard, J. Marien, L. Kocon, J.-N. Rouzaud, F. Béguin, J.-P. Pirard, Carbon **43** (2005) 2481.
[13] C. Moreno-Castilla, F.J. Maldonado-Hódar, Carbon **43** (2005) 455.
[14] N. Job, B. Heinrichs, S. Lambert, J.-P. Pirard, J.-F. Colomer, B. Vertruyen, J. Marien, AIChE J. 52 (2006) 2663.
[15] P.V. Samant, M.F.R. Pereira, J.L. Figueiredo, Catal. Today **102-103** (2005) 183.
[16] J. Marie, S. Berthon-Fabry, P. Achard, M. Chatenet, A. Pradourat, E. Chainet, J. Non-Cryst. Solids **350** (2004) 88.
[17] J. Marie, S. Berthon-Fabry, M. Chatenet, E. Chainet, R. Pirard, N. Cornet, P. Achard, J. Appl. Electrochem. **37** (2007) 147.
[18] N. Job, J. Marie, S. Lambert, S. Berthon-Fabry, P. Achard, Energ. Convers. Manage. **49** (2008) 2461.
[19] J. Marie, R. Chenitz, M. Chatenet, S. Berthon-Fabry, N. Cornet, P. Achard, J. Power Sources (2009), in press.
[20] C. Arbizzani, S. Beninati, E. Manferrari, F. Soavi, M. Mastragostino, J. Power Sources **172** (2007) 578.
[21] N. Job N, M.F.R. Pereira, S. Lambert, A. Cabiac, G. Delahay, J.-F. Colomer, J. Marien, J.L. Figueiredo, J.-P. Pirard, J. Catal. **240** (2006) 160.

[22] J.R. Regalbuto, in *Catalyst Preparation: Science and Engineering*; Regalbuto, J.R., Ed.; CRC Press, Taylor & Francis Group, Boca Raton (FL), 2007, p. 297.
[23] S. Lambert, N. Job, L. D'Souza, M.F.R. Pereira, R. Pirard, B. Heinrichs, J.L. Figueiredo, J.-P. Pirard, J.R. Regalbuto, J. Catal. **261** (2009) 23.
[24] N. Job, S. Lambert, M. Chatenet, C.J. Gommes, F. Maillard, S. Berthon-Fabry, J.R. Regalbuto, J.-P. Pirard, Catal. Today, submitted.
[25] N. Job, F. Maillard, J. Marie, S. Berthon-Fabry, J.-P. Pirard, M. Chatenet. J. Mater. Sci. (2009), in press.
[26] S. Trasatti, J. Electroanal. Chem. **327** (1992) 353.
[27] F. Maillard, M. Eikerling, O.V. Cherstiouk, S. Schreier, E. Savinova, U. Stimming, Faraday Discuss. **125** (2004) 357.
[28] F. Maillard, S. Schreier, M. Hanzlik, E.R. Savinova, S. Weinkauf, U. Stimming, Phys. Chem. Chem. Phys. **7** (2005) 385.
[29] F. Maillard, E.R. Savinova, U. Stimming, J. Electroanalytical Chem. **599** (2007) 221.
[30] B. Andreaus, F. Maillard, J. Kocylo, E. R. Savinova, M. Eikerling, J. Phys. Chem. B **110** (2006) 21028.
[31] H.H. Holscher, W.M.H. Sachtler, Discuss. Faraday Soc. **41** (1966) 29.
[32] H.A. Gasteiger, W. Gu, R. Makharia, M.F. Mathias, B. Sompalli, in *Handbook of Fuel Cells – Fundamentals, Technology and Applications*; Vielstich, W., Lamm, A., Gasteiger, H.A., Eds.; Wiley, Chichester (UK), 2003, Vol. 3, p. 593.
[33] H.A. Gasteiger, S.S. Kocha, B. Sompalli, F.T. Wagner, Appl. Catal. B **56** (2005) 9.
[34] S.D. Thompson, L.R. Jordan, M. Forsyth, Electrochim. Acta **46** (2001) 1657.